Phase diagram of the t-U-V_1-V_2 model at quarter filling

Satoshi Ejima,[1] Florian Gebhard,[1] Satoshi Nishimoto,[2] and Yukinori Ohta[3]
[1]*Fachbereich Physik, Philipps-Universität Marburg, D-35032 Marburg, Germany*
[2]*Institute for Theoretical Physics, University of Göttingen, D-37077 Göttingen, Germany*
[3]*Department of Physics, Chiba University, Chiba 263-8522, Japan*
(Received 4 November 2004; revised manuscript received 21 January 2005; published 5 July 2005)

We examine the ground-state properties of the one-dimensional Hubbard model at quarter filling with Coulomb interactions between nearest-neighbors V_1 and next-nearest neighbors V_2. Using the density-matrix renormalization group and exact diagonalization methods, we obtain for $U=10t$ three different phases in the V_1-V_2 plane: $2k_F$- and $4k_F$-charge-density-wave (CDW) and a broad metallic phase in between. Assuming that the metal is a Tomonaga-Luttinger liquid (TLL), we calculate the TLL parameter K_ρ. It is largest when V_1 and V_2 are frustrated, and $K_\rho=0.25$ at the boundaries between the metallic phase and each of the two CDW phases.

DOI: 10.1103/PhysRevB.72.033101 PACS number(s): 71.10.Fd, 71.30.+h, 71.10.Hf

The low-energy physics of one-dimensional correlated electron system can be described by the Tomonaga-Luttinger liquid theory.[1] In general, the Green function and various correlation functions show a power-law behavior as a function of momentum k and frequency ω. The decay of the correlation functions is determined by the so-called TLL parameter K_ρ that depends on the strength of the interactions. Numerous experiments as well as theoretical studies have been performed on a variety of systems in order to determine K_ρ for one-dimensional metallic systems.

Most features of a recent angle-resolved photoemission spectroscopy (ARPES) experiment for the quasi-one-dimensional organic conductor TTF-TCNQ[2] can be explained by the photoemission spectral function of the one-dimensional Hubbard model with only on-site interaction.[3] However, the Hubbard model yields $K_\rho \geqslant 0.5$, in contrast to $K_\rho \simeq 0.18$ as deduced from angle-integrated data for the density of states,[2] which suggest a power-law behavior of the density of states near the Fermi level, $\rho(\omega) \propto \omega^\alpha$, where $\alpha = (K_\rho + K_\rho^{-1} - 2)/4$ with $\alpha \simeq 1$. Another example of a small K_ρ is the quasi-one-dimensional organic conductor $(TMTSF)_2X$, where $X = PF_6$, ASF_6, or ClO_4. In this system, the parameter K_ρ was estimated to be $K_\rho \simeq 0.23$ from the power-law dependence dominating in the higher-energy part of the optical conductivity, $\sigma(\omega) \sim \omega^{4a^2K_\rho - 5}$, where a is the order of the commensurability ($a=1$ for half filling; $a=2$ for quarter filling).[4,5] This value is consistent with ARPES measurements.[6] TLL behavior was also suggested for the strongly anisotropic transition-metal oxide $PrBa_2Cu_4O_8$; the parameter was estimated to be $K_\rho \simeq 0.24$ from both the optical conductivity[7] and the ARPES study of Zn-doped $PrBa_2Cu_4O_8$.[8,9]

Common features of all the materials mentioned above are that the filling of the conduction band is near one-quarter, $n \simeq 0.5$.[2,7,8,10,11] Consequently, they are close to a charge-density-wave (CDW) instability.[12–15] In addition, the parameter K_ρ is rather small, which is incompatible with the result from a simple one-dimensional Hubbard model and shows that the long-range Coulomb interactions between carriers is relevant. Therefore, we examine the one-dimensional Hubbard model with interactions to nearest and next-nearest neighbors,

$$\begin{aligned}\hat{H} = &- t\sum_{i,\sigma} (\hat{c}^\dagger_{i,\sigma}\hat{c}_{i+1,\sigma} + \text{H. c.}) + U\sum_i \hat{n}_{i,\uparrow}\hat{n}_{i,\downarrow} \\ &+ V_1 \sum_{i,\sigma\sigma'} \left(\hat{n}_{i,\sigma} - \frac{1}{2}\right)\left(\hat{n}_{i+1,\sigma'} - \frac{1}{2}\right) \\ &+ V_2 \sum_{i,\sigma\sigma'} \left(\hat{n}_{i,\sigma} - \frac{1}{2}\right)\left(\hat{n}_{i+2,\sigma'} - \frac{1}{2}\right), \end{aligned} \tag{1}$$

where $\hat{c}^\dagger_{i,\sigma}(\hat{c}_{i,\sigma})$ is the creation (annihilation) operator of an electron with spin $\sigma(=\uparrow,\downarrow)$ at site i and $\hat{n}_{i,\sigma} = \hat{c}^\dagger_{i,\sigma}\hat{c}_{i,\sigma}$ is the number operator. t is the hopping integral between neighboring sites, U is the strength of the Hubbard interaction, and the charge frustrating interactions V_1 and V_2 determine the nearest-neighbor and next-nearest-neighbor Coulomb repulsion. We restrict ourselves to the case of quarter filling ($n=1/2$) and strong coupling, $U=10t$.

So far, several theoretical studies have been made on this and similar models.[16–21] In the ground state there exist two CDW phases with wave numbers $q=2k_F$ and $4k_F$. Between the two CDW phases there appears a wide region of a vanishing charge gap that results from the geometrical frustration of the long-range Coulomb interactions. If we assumed the intersite Coulomb repulsions to be inversely proportional to the intersite distance, we would find $V_1=2V_2$, so that neither of the two CDW instabilities dominates in the atomic limit, $t=0$. Hence, one can easily imagine that the phase diagram contains a metallic region as soon as a finite t is introduced. However, little is known about the physical properties of this metallic state. It is our purpose in this paper to obtain an accurate ground-state phase diagram of the t-U-V_1-V_2 model, including the TLL parameter K_ρ whereby we make the natural assumption that the metallic phase is a Tomonaga-Luttinger liquid. Our phase diagram is shown in Fig. 1.

We apply the density-matrix renormalization group (DMRG) method for the calculation of the ground-state energy. We study chains with up to 256 sites with open boundary conditions and keep up to $m=2000$ density-matrix eigenstates so that the maximum truncation error is about 10^{-5}. We

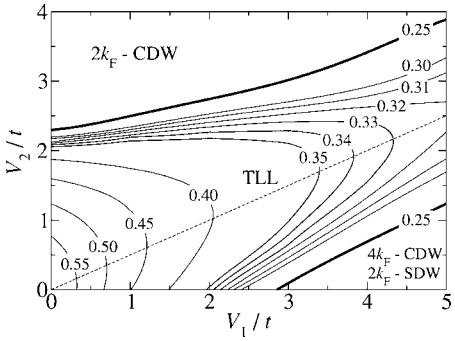

FIG. 1. Phase diagram of the one-dimensional t-U-V_1-V_2 model for $U=10t$ at quarter filling. The curves show the contours of constant TLL parameter K_ρ. Bold lines represent the boundary of the metal-insulator (CDW) transition and the dotted line corresponds to $V_2/t=V_1/(2t)$.

use periodic boundary conditions for the calculation of charge excitations with the Lanczos exact diagonalization technique.

In order to determine the metallic region in the phase diagram, we calculate the two-particle charge gap,

$$\Delta_c^{(2)}(L) = E_0(N_\uparrow+1,N_\downarrow+1,L) + E_0(N_\uparrow-1,N_\downarrow-1,L) - 2E_0(N_\uparrow,N_\downarrow,L), \quad (2)$$

where $E_0(N_\uparrow,N_\downarrow,L)$ denotes the ground-state energy of a chain of length L with $N_\uparrow$ spin-up electrons and $N_\downarrow$ spin-down electrons. When pairing is absent, in the thermodynamic limit the two-particle charge gap becomes twice the single-particle charge gap, $\lim_{L\to\infty}\Delta_c^{(2)}(L)=2\lim_{L\to\infty}\Delta_c(L)$. We find that $\Delta_c^{(2)}(L)$ decreases monotonically with increasing L, so that we can extrapolate it to the thermodynamic limit systematically by performing a polynomial fitting in $1/L$. Note that we need relatively large system sizes to obtain an accurate phase boundary. The extrapolated results $\Delta_c^{(2)}/t$ at $U/t=10$ and $V_1/t=4$ are shown in Fig. 2.

It is evident that $\Delta_c^{(2)}/t$ is finite for both small $V_2/t \leqslant 0.66$ and large $V_2/t \geqslant 3.43$, i.e., the system is insulating, and $\Delta_c^{(2)}/t$ vanishes in a wide range of V_2/t, i.e., $0.66 \leqslant V_2/t \leqslant 3.43$, within the accuracy of the extrapolation (error smaller than $10^{-4}t$). We find similar situations for other values of V_1/t as well, which demonstrates that a stable metallic phase indeed exists between two insulating phases, as shown in Fig. 1. This result is consistent with other studies.[17–21]

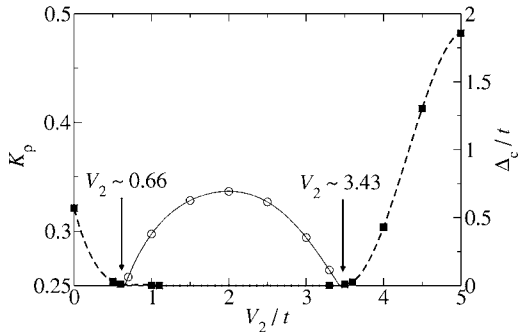

FIG. 2. Charge gap $\Delta_c^{(2)}/(2t)$ (squares) and TLL parameter K_ρ (circles) in the one-dimensional t-U-V_1-V_2 model at quarter filling for $U/t=10$ and $V_1/t=4$. Lines are guides to the eye.

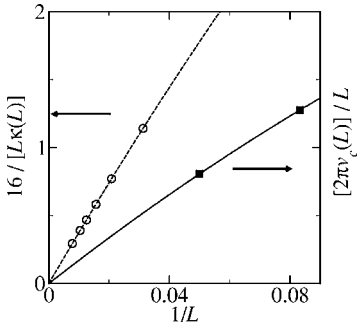

FIG. 3. Scaling of the ground-state energy differences from Eq. (4) and the excitation energy from Eq. (5) as a function of $1/L$ at $U/t=10$, $V_1/t=1$ and $V_2/t=1$. The lines indicate the polynomial fits by Eq. (6) to the data.

In the Tomonaga-Luttinger phase, the dominant correlations are determined by a single parameter K_ρ, which is given by[22–24]

$$K_\rho = (\pi/2)n^2\kappa v_c, \quad (3)$$

where κ and v_c are the compressibility and the charge velocity, respectively. To estimate K_ρ numerically, we calculate the compressibility κ from the charge gap,

$$\Delta_c^{(2)}(L) = 4/[n^2 L\kappa(L)], \quad (4)$$

and the velocity of the charge excitations v_c from

$$E_{1\rho}(N_\uparrow,N_\downarrow,L) - E_0(N_\uparrow,N_\downarrow,L) = 2\pi v_c(L)/L, \quad (5)$$

where $E_{1\rho}(N_\uparrow,N_\downarrow,L)$ is the lowest excitation energy with momentum $k=2\pi/L$ and total spin $S=0$ for finite system size L. As shown in Fig. 3, both of the quantities are monotonous functions of $1/L$ for all parameter sets and can be fitted to a polynomial function,

$$f(L) = a_1 L^{-1} + a_2 L^{-2} + \cdots. \quad (6)$$

Therefore, we obtain

$$\kappa = \lim_{L\to\infty}\kappa(L) = 16/a_1^{(\kappa)}, \quad (7)$$

$$v_c = \lim_{L\to\infty} v_c(L) = a_1^{(v_c)}/2\pi, \quad (8)$$

so that the TLL parameter can be estimated as

$$K_\rho = a_1^{(v_c)}/a_1^{(\kappa)} \quad (9)$$

in the thermodynamic limit. For the compressibility we can use DMRG for up to 128 sites. The extrapolation is very well behaved, and a reliable extrapolation could have been obtained from the results for much smaller systems. This makes us confident that the extrapolation for the charge velocity is meaningful despite the fact that exact diagonalization is limited to $L \leqslant 20$. A comparison with the exact K_ρ^{exact} for the one-dimensional Hubbard model[22] shows that relative errors $|K_\rho^{\text{DMRG}} - K_\rho^{\text{exact}}|/K_\rho^{\text{exact}}$ are below 1%. For finite V_1 and/or V_2,

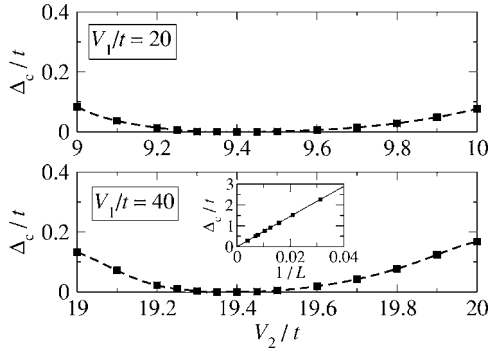

FIG. 4. Charge gap for spinless fermions at $V_1/t=20$ (upper part) and $V_1/t=40$ (lower part). The charge gap vanishes around $V_2/t=V_1/(2t)-0.6$ in both cases. The inset shows the charge gap for $V_2/t=19.4$ as a function of $1/L$ for system sizes up to $L=256$.

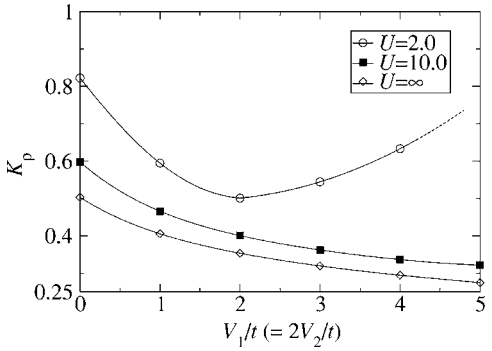

FIG. 5. TLL parameter K_ρ of the t-U-V_1-V_2 model at quarter-filling as a function of V_1/t along a line $V_1=2V_2$ for $U=2t$ (circles), $U=10t$ (squares), and $U=\infty$ (diamonds). The lines are guides to the eye.

our results are consistent with other estimates using the charge structure factor.[25–27]

In Fig. 2, the parameter K_ρ is plotted as a function of V_2/t at fixed $U/t=10$ and $V_1/t=4$. We see that $K_\rho>0.25$ when the charge gap is zero and $K_\rho=0.25$ at the critical points. We have confirmed numerically that K_ρ is always 0.25 at the CDW critical points for all finite values of U. K_ρ reaches its maximum value around $V_1=2V_2$, i.e., the density-density correlations decay most rapidly when V_1 and V_2 maximally frustrate each other. In general, long-range Coulomb repulsions are expected to suppress the value of K_ρ. This is consistent with our results because K_ρ decreases when the values of V_1 and V_2 deviate from the relation $V_1\approx 2V_2$, whereby the effective interaction strength increases. Apparently, the line $V_1=2V_2$ goes along the ridges of the contour line of K_ρ in Fig. 1. This has been already suggested in the spinless fermion case and similar models.[19,21]

In the limit of large values of V_1 and $V_2(V_1,V_2<U)$, the boundary between the ordered phases and the metallic phase shrinks. In Fig. 4, we show the charge gap as a function of V_2/t at $V_1/t=20$ and $V_1/t=40$ for spinless fermions ($U=\infty$). It demonstrates that a narrow but stable metallic regime exists between the two insulating phases. For large V_1 and V_2 it is very difficult to extrapolate $\Delta_c^{(2)}$ reliably from exact diagonalization data ($L\leqslant 20$), and DMRG [$L\sim\mathcal{O}(200)$] must be used in the extrapolation. For example, Fig. 4 shows that $V_1/t=40$ at $V_2/t=20$ is a CDW insulator whereas it has been assigned a "non-Tomonaga-Luttinger metal" in Ref. 20. Even with DMRG it is very difficult to decide whether or not the metallic region shrinks to zero at some tricritical point, as proposed in Ref. 21. If it exists it is far beyond the values quoted previously.[21] As seen from Fig. 4 there is a metallic region for $V_1/t=40$ in the vicinity of $V_2/t=19.4$. In the surrounding of this point, the gap nicely scales to zero as a function of the inverse system size, as seen from the inset to Fig. 4. Our results indicate that the metallic phase appears below the line $V_2=V_1/2$, around $V_2=V_1/2-0.6t$. We speculate that there is a metallic phase between the two CDW phases for all finite V_1 and V_2, i.e., there are no tricritical points in the V_1-V_2 phase diagram.

In order to study the spin degrees of freedom, we calculate the spin gap for system size L, defined by

$$\Delta_s(L) = E_0(N_\uparrow+1, N_\downarrow-1, L) - E_0(N_\uparrow, N_\downarrow, L). \qquad (10)$$

As in the case of charge gap, the extrapolation to the thermodynamic limit is straightforward. In the $2k_F$-CDW phase, we find that Δ_s is always finite because the system contains separated spin singlet pairs. For fixed V_1, Δ_s increases as a function of V_2 and eventually saturates at $\Delta_s=4t^2/(U-V_1)$ in the limit $V_2\to\infty$. This is readily understood because, for $U, V_2 \gg V_1$, the system can be mapped to an effective spin Hamiltonian $H=J_{2k_F}\Sigma_i \hat{\mathbf{S}}_{4i}\cdot\hat{\mathbf{S}}_{4i+1}$ with $J_{2k_F}=4t^2/(U-V_1)$. This model is trivial and the spin gap is the energy difference between the singlet and triplet state at each bond, $\Delta_s=4t^2/(U-V_1)$.

In the $4k_F$-CDW phase, we find that Δ_s is always zero, because a charged site and a vacant site come alternately and the spin degrees of freedom can be described in terms of a one-dimensional uniform Heisenberg model. In fact, for $U>V_1/2\gg V_2$, the effective spin Hamiltonian can be written as $H=J_{4k_F}\Sigma_i \hat{\mathbf{S}}_{2i}\cdot\hat{\mathbf{S}}_{2i+2}$ with $J_{4k_F}=4(t^2/(V_1-2V_2))^2[1/(U-V_2)+2/(U-2V_2)]$. This effective Heisenberg model displays gapless spin excitations, in agreement with our numerical results.

Lastly, we plot the TLL parameter K_ρ as a function of V_1/t for fixed $V_1=2V_2$ and several values of U in Fig. 5. For large U, K_ρ decreases as a function of V_1/t and eventually crosses $K_\rho=0.25$ at some finite value of $V_{1,c}$. As shown above, $K_\rho\geqslant 0.25$ for a metallic phase, so that the Tomonaga-Luttinger liquid turns into the $4k_F$-CDW at $V_{1,c}$. For small U, e.g., $U=2t$ in Fig. 5, K_ρ decreases as a function of V_1, displays a minimum around $V_1/t\approx\mathcal{O}(U/t)$ with $K_{\rho,\min}>0.25$, and increases again. This results from the fact that V_1 overcomes the Hubbard interaction U and electrons with opposite spin gain energy from on-site pairing. Eventually, K_ρ can become larger than unity and superconducting correlations are dominant. As seen from Fig. 5, the ground-state phase diagram in Fig. 1 is representative for all $U\gtrsim 4t$ when a superconducting phase does not interfere. The ridge of K_ρ goes along the line $V_1=2V_2$ and K_ρ decreases as the value of V_1 and V_2 deviates from this line.

In conclusion, we obtained an accurate ground-state phase diagram of the t-U-V_1-V_2 model at quarter-filling using DMRG and exact diagonalization methods. For intermediate to large Hubbard interaction $U \gtrsim 4t$, the system has CDW phases with $q=2k_F$ and $4k_F$ between which there appears a broad region of a Tomonaga-Luttinger liquid. Because of the geometrical frustration of the long-range Coulomb interactions, K_ρ is maximum around $V_2=V_1/2$. It is smallest at the phase boundaries, $K_\rho=0.25$, which appears to be universal for transitions between the metallic and the CDW phases.[21]

We are grateful to E. Jeckelmann, G. Japaridze, and P. Schmitteckert for helpful discussions. We acknowledge support by the Central Institute for Applied Mathematics at Research Centre Jülich. S.E. is supported by the Honjo International Scholarship Foundation. Also acknowledged is partial support by Grants-in-Aid for Scientific Research from the Ministry of Education, Science, Sports, and Culture of Japan. A part of the computations was carried out at the computer centers of the Institute for Molecular Science, Okazaki, and the Institute for Solid State Physics, University of Tokyo.

[1] K. Schönhammer, in *Strong Interactions in Low Dimensions, Physics and Chemistry of Materials with Low-Dimensional Structures*, edited by D. Baeriswyl and L. Degiorgi (Springer-Verlag, Berlin, 2004), vol. 25; "Luttinger liquids: The basic concepts," *Interaction g Electrons in Low Dimensions* (Kluwer Academic, New York, 2003).
[2] R. Claessen, M. Sing, U. Schwingenschlögl, P. Blaha, M. Dressel, and C. S. Jacobsen, Phys. Rev. Lett. **88**, 096402 (2002).
[3] H. Benthien, F. Gebhard, and E. Jeckelmann, Phys. Rev. Lett. **92**, 256401 (2004).
[4] V. Emery, in *Highly Conducting One-Dimensional Solids*, edited by J. T. Devreese *et al.* (Plenum, New York, 1979), p. 327.
[5] J. Sólyom, Adv. Phys. **28**, 209 (1979).
[6] F. Zwick, S. Brown, G. Margaritondo, C. Merlic, M. Onellion, J. Voit, and M. Grioni, Phys. Rev. Lett. **79**, 3982 (1997).
[7] K. Takenaka, K. Nakada, A. Osuka, S. Horii, H. Ikuta, I. Hirabayashi, S. Sugai, and U. Mizutani, Phys. Rev. Lett. **85**, 5428 (2000).
[8] T. Mizokawa, A. Ino, T. Yoshida, A. Fujimori, C. Kim, H. Eisaki, Z.-X. Shen, S. Horii, T. Takeshita, S. Uchida, K. Tomimoto, S. Tajima, and Y. Yamada, in *Stripes and Related Phenomena*, edited by A. Bianconi and N. L. Saini (Plenum, New York, 2000).
[9] T. Mizokawa, K. Nakada, C. Kim, Z.-X. Shen, T. Yoshida, A. Fujimori, S. Horii, Y. Yamada, H. Ikuta, and U. Mizutani, Phys. Rev. B **65**, 193101 (2002).
[10] M. Sing, U. Schwingenschlögl, R. Claessen, P. Blaha, J. M. P. Carmelo, L. M. Martelo, P. D. Sacramento, M. Dressel, and C. S. Jacobsen, Phys. Rev. B **68**, 125111 (2003).
[11] C. Bourbonnais and D. Jérome, *Advances in Synthetic Metals, Twenty Years of Progress in Science and Technology*, edited by P. Bernier, S. Lefrant, and G. Bidan (Elsevier, New York, 1999), p. 206.
[12] R. Claessen (private communication, 2004).
[13] F. Nad, P. Monceau, C. Carcel, and J. M. Fabre, Phys. Rev. B **62**, 1753 (2000).
[14] D. S. Chow, F. Zamborszky, B. Alavi, D. J. Tantillo, A. Baur, C. A. Merlic, and S. E. Brown, Phys. Rev. Lett. **85**, 1698 (2000).
[15] S. Fujiyama, M. Takigawa, and S. Horii, Phys. Rev. Lett. **90**, 147004 (2003).
[16] H. Yoshioka, M. Tsuchiizu, and Y. Suzumura, J. Phys. Soc. Jpn. **70**, 762 (2001).
[17] D. Poilblanc, S. Yunoki, S. Maekawa, and E. Dagotto, Phys. Rev. B **56**, R1645 (1997).
[18] H. Seo and M. Ogata, Phys. Rev. B **64**, 113103 (2001).
[19] S. Nishimoto and Y. Ohta, Phys. Rev. B **68**, 235114 (2003).
[20] A. K. Zhuravlev, M. I. Katsnelson, and A. V. Trefilov, Phys. Rev. B **56**, 12939 (1997); A. K. Zhuravlev and M. I. Katsnelson, *ibid.* **61**, 15534 (2000).
[21] P. Schmitteckert and R. Werner, Phys. Rev. B **69**, 195115 (2004).
[22] H. J. Schulz, Phys. Rev. Lett. **64**, 2831 (1990).
[23] N. Kawakami and S.-K. Yang, Phys. Lett. A **148**, 359 (1990).
[24] H. Frahm and V. E. Korepin, Phys. Rev. B **42**, 10553 (1990).
[25] S. Daul and R. M. Noack, Phys. Rev. B **58**, 2635 (1998).
[26] R. T. Clay, A. W. Sandvik, and D. K. Campbell, Phys. Rev. B **59**, 4665 (1999).
[27] S. Ejima, S. Nishimoto, and F. Gebhard, Europhys. Lett. **70**, 492 (2005).